Korean J. Chem. Eng., 32(6), 1151-1157 (2015)
DOI: 10.1007/s11814-014-0312-z

pISSN: 0256-1115
eISSN: 1975-7220

Experimental and theoretical investigation of a new multistage countercurrent melt crystallizer with inclined sieve plates

Shui Wang*, Guojing Zhao*, Yizhen Du, and Yixin Qu**,†**

*Beijing Key Laboratory of Membrane Science and Technology, College of Chemical Engineering, Beijing University of Chemical Technology, Beijing 100029, P. R. China
**Shandong Academy of Environmental Science, Jinan 250013, P. R. China
(*Received 16 February 2014 • accepted 16 October 2014*)

Abstract−A new multistage countercurrent melt crystallizer with sieve plates is proposed that combines the advantages of the TNO column crystallizer and the inclined column crystallizer. With the naphthalene-indene solid solution system, the purification process of organic materials in the new multistage countercurrent melt crystallizer with sieve plates under total reflux was investigated. Two of the influencing factors on the separation and purification performance in the new multistage countercurrent melt crystallizer with sieve plates were crystal settling velocity and crystal breakage, which were controlled by stirring speed, the sieve plates, the angle of the sieve plates, the diameter of the pores, particle sedimentation area, and the number of plates. The results of this study show that the optimum stirring speed was determined to be 20 rpm, sieve plates can obviously increase the separation and purification effect, the optimum angle of the sieve plates was determined to be 45°, the optimum diameter of the pores was determined to be 8 mm, the optimum particle sedimentation area was determined to be 0.5 r, and two plates in the crystallizer were shown to be the best.

Keywords: Melt Crystallizer, Sieve Plates, Separation, Purification

INTRODUCTION

Melt crystallization facilitates the ultrapurification of organic compounds at relatively low energy consumption compared to distillation, while the use of solvent as in extraction is avoided. Countercurrent column crystallization is a rather efficient and promising method for the separation and purification of substances. Currently, a number of large scale processes involve countercurrent crystallization (wash) columns of different (mechanical, hydraulic, gravity) types and scales. The process has also been the subject of many experimental studies and model formulation [1-4].

TNO has developed a new crystallization column in which the countercurrent contact between crystals and melts is promoted by exerting a mechanical action to enhancing crystal breakage on the crystals [5]. The purifier is a column with a number of sieve trays attached to a central shaft that oscillates up and down. As the slurry flows through the tower, bouncing balls on each tray impact the crystals and break up some of them. The resulting small crystals melt and enrich the liquid phase, thus providing an upward refluxing action on the large crystals that continue downward to the melting zone at the bottom. Reflux is returned from the melting zone and product is taken off. For the separation of benzene and thiophene that form a solid solution, a tray efficiency of more than 40% could be realized. Flow rates of 100-1,000 kg/m^2 hr have been tested. The residence time of crystals was about 30 min per stage. Eutectic systems also have been handled satisfactorily. A column 500 mm dia and 3 m long with 19 trays has been built; it is expected to have a capacity of 300 tons/yr., but construction of the column is rather complicated, and the scaling up of the process is difficult.

Matsuoka et al. proposed a common type of inclined column crystallizer that enhances countercurrent contact between crystals and melts by inclining the column crystallizer [6]. In classical settlement theory the crystal settling velocity mainly depends on grain diameter, the density difference between solid and liquid, and the viscosity of suspending liquid. And later, the researcher Boycott in blood sedimentation test found that the blood sedimentation rate increases significantly if the blood test tube is inclined. This phenomenon is referred to as the Boycott effect [7]. The crystallizer consists of three sections for crystallization, purification, and melting. The crystallization section has a jacket for the flow of coolant, the temperature of which is controlled by a thermostatic bath. The melting section has a heater to melt crystals, and the heating power can be adjusted by a voltage regulator. Crystals are produced in the crystallization section and move to the melting section by gravity and stirring. Crystals are purified in the purification section and are melted in the melting section; the movement of crystals is enhanced by tilting the column. The purification section is insulated by glass wool to obtain approximately adiabatic conditions. The device is still at the laboratory research stage at present. Matsuoka studied the crystallizer at total reflux, Funakoshi et al. [8] studied the reflux ratio on separation and purification performance of the crystallize, and Chen et al. [9] performed a systematic study on the operation of inclined column crystallizer.

In this paper, a new column crystallizer is introduced combined

†To whom correspondence should be addressed.
E-mail: yxqu2008@163.com

with the advantage of the inclined column crystallizer and the TNO crystallizer. It absorbs the advantages of promoting the settlement of solid particles that the inclined column crystallizer possesses. At the same time, it absorbs the advantage of strengthening heat and mass transfer, and crystal breakage that TNO column crystallization has. So this new column crystallizer is better with respect to mass and heat transfer, and can easily solve problems associated with solid particle sedimentation. The separation experiment was conducted in a top-fed column and purified naphthalene-indene system that naphthalene as the main separation component by the new multistage countercurrent melt crystallizer with sieve plate under total reflux.

THEORY

There are three purification mechanisms in the melt crystallization: recrystallization, washing, and sweating. The washing mechanism is a convective diffusion between crystal and melt owing to their differential concentration, which facilitates successful heat and mass transfer. The washing mechanism in the purification section is displayed in Eq. (1). It is assumed that M_k is proportional to the differential concentration between crystalline particles and reflux melts.

$$M_k=K_a\rho_L A(w_s-w_L)\Delta z \tag{1}$$

where K_a denotes the mass transfer coefficient between crystalline particles and reflux melts.

Axial dispersion models are generally accepted, but do not consider the sweating effect and assume that crystal composition is constant along axis [9-12]. For systems involving organic materials, the crystal size is relatively small, and the crystallizer is operated at temperature near the melting point, so it is reasonable to consider sweating effects. The composition change in the crystal phase is assumed to be caused by the sweating mechanism, whereby composition changes occur when the crystals are subjected to a temperature closer to the melting point (equilibrium point for solid solution systems) than the temperature at which the crystals are formed [13,14]. Assuming a similar expression for the composition change of the solid phase, the purification rate [15,16] can be written as

$$\frac{dw_s}{d\theta}=kA(w_s^*-w_s) \tag{2}$$

For a eutectic system, $w_S^*=1$. Because the feed concentration in the study is relatively high ($w_F=0.85$), the assumption $w_S^*\approx 1$ can be made.

Mathematical analyses of column crystallization are mainly made for the purification section [17-19], but recrystallization mainly occurs in the crystallization section, so its effect is generally ignored.

Before the model is formulated, some assumptions should be made:

(1) The column crystallizer has attained thermal equilibrium.

(2) The crystal flux and melt flux are ideal piston flow.

(3) The solid flux S, the melt flux L, and the axial dispersion coefficient are constant throughout the column.

(4) The flow rate of melts is proportional to the flow rate of the crystals.

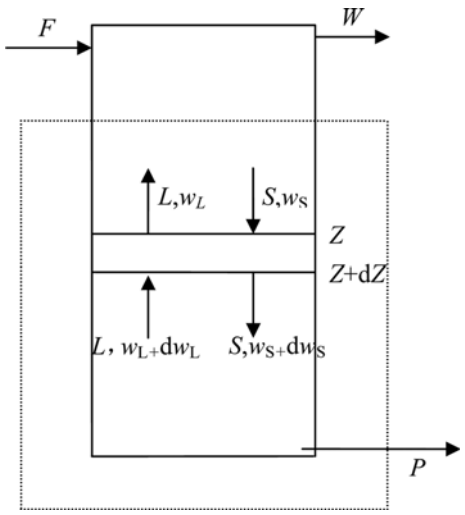

Fig. 1. Elemental description of the column crystallizer.

(5) The sieve plates enhance heat and mass transfer, leading to the purification mechanism described as Eq. (1).

Theoretical studies were conducted on the new multistage countercurrent melt crystallizer with sieve plates as shown in Fig. 1.

The total mass balance is given by

$$S-L-P=0 \tag{3}$$

The component mass balance is

$$Sw_s-Lw_L-Pw_P=0 \tag{4}$$

The mass balance over a volume element at z is given by

$$Sdw_s=Ldw_l=M_k dA=k(w_s^*-w_s)\alpha(1-\phi)Adz \tag{5}$$

if

$$K=k\alpha(1-\phi)A \tag{6}$$

then

$$Sdw_s=Ldw_l=M_k dA=K(1-w_s)dz \tag{7}$$

$$\frac{Sdw_s}{(1-w_s)}=\frac{Ldw_L}{(1-w_s)}=Kdz \tag{8}$$

The boundary conditions are given by

$$z=0 \qquad w_S=w_{S_0}$$

By Eq. (8), the following equation can be obtained

$$\ln\frac{1-w_S}{1-w_{S_0}}=-\frac{K}{S}z \tag{9}$$

By Eq. (4), w_s is given by

$$w_S=\frac{Lw_L+Pw_P}{L+P} \tag{10}$$

By combining Eqs. (1), (9) and (10), the following equation can be obtained:

$$\ln\frac{L+P-Lw_L-Pw_P}{L+P-Lw_{L0}-Pw_P}=-\frac{K}{L+P}z \tag{11}$$

If ignoring the influence of axial diffusion in microcosmic material balance, the model can be introduced in Eq. (12).

$$\ln\frac{w_L-a}{w_{L0}-a}=\ln\frac{a-w_L}{a-w_{L0}}=-bz \tag{12}$$

where

$$a=\frac{L+P-Pw_P}{L}$$

$$b=\frac{K}{L+P}$$

It indicates that $\ln(a-w_L)$, should decrease linearly with the position z in the purification section.

For total reflux, P=0, a=1, Eq. (12) can be written as

$$\ln\frac{w_L-1}{w_{L0}-1}=\ln\frac{1-w_L}{1-w_{L0}}=-bz \tag{13}$$

Replacing $1-w_L$ by y, yields

$$\ln y=\ln y_0-bz \tag{14}$$

Eq. (14) indicates that should decrease linearly with the position z in the purification section under total reflux, with the intercept $\ln y_0$, the slope, $-b$.

EXPERIMENT

1. Apparatus

A schematic diagram of a new column crystallizer with sieve plates is illustrated in Fig. 2(a) and (b). The crystallizer made of glass was 700 mm in height and 50 mm in inner diameter. It had a stirrer with several scrapers made of stainless steel and weld on the shaft, which was driven by a stepper motor to prevent encrustation on the column walls and to enhance the countercurrent contact between the crystalline particles and reflux melts.

The crystallizer consists of three sections for crystallization, purification, and melting. The crystallization section has a jacket for

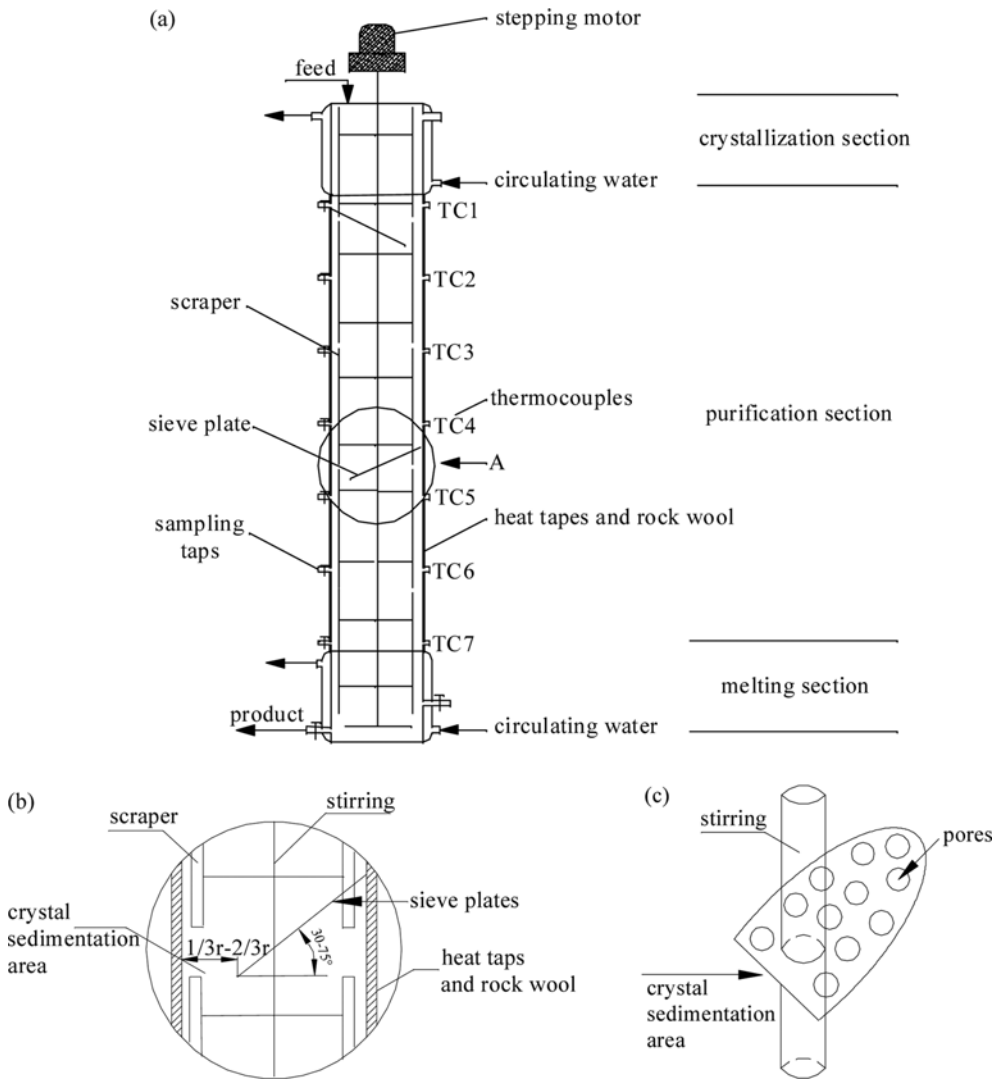

Fig. 2. (a) Schematic diagram of the new multistage countercurrent melt crystallizer with sieve plates. (b) Partial enlarged drawing of part A in Fig. 1. (c) The shape of sieve plate.

the flow of coolant, the temperature of which is controlled by a thermostatic bath. The melting section also has a jacket for the flow of hot water, the temperature of which is controlled by a constant temperature circulation water bath. Crystals are produced in the crystallization section and moved to the melting section by gravity and stirring. Crystals are purified in the purification section and melted in the melting section. The purification section is wrapped by heat tapes and rock wool to keep the experimental column approximately at a constant temperature. Inside the crystallizer, several sieve plates are fixed on the rotation to enhance heat and mass transfer, and crystal breakage in the purification. Unlike the TNO column, this column does not have balls on the trays, and the sieve plates absorb the advantage of inclined crystallizer. When the sieve plates are allowed to incline, they facilitate the settlement of solid particles, and absorb the advantage of TNO column crystallizer, with the ability of strengthening the mass transfer, heat transfer and particle breaking. The shape of the sieve plates is shown in Fig. 2(c).

There were seven sampling taps on one side of the new crystallizer to sample the melts and measure the composition, while on the other side of the crystallizer are corresponding temperature taps to monitor the temperature. Temperatures were measured by thermal resistance and displayed on a multichannel temperature display and control system. Samples of melts were removed by turning the valves open. Experiments were carried out in the manner of total reflux to observe the purification effect under different conditions.

2. Methods

The solid solution naphthalene-indene system was chosen for this study. All experiments were conducted with naphthalene as the major component. The mass fraction was 0.85. Before the experiment, the hot water was preheated at 83.3 °C, and the heat tapes at 50 °C, while the stepper motor was set at 20 rpm. First, the crystal was heated to liquid until the second taps, and then added from the top of the crystallizer. The experiment commenced when the bottom of the crystallizer appeared crystal. Samples were withdrawn every 10 min. The operations underwent total reflux for 1 hour until the bottom of this new crystallizer appeared crystal. The samples were analyzed by flame ionization detector (FID) gas chromatography. The crystal settling velocity and crystal breakage were controlled by stirring speed, the sieve plates, the angle of sieve plates, the diameter of pores, the particle sedimentation area, and the number of plates.

RESULTS AND DISCUSSION

We chose the naphthalene-indene system; naphthalene was white crystal, indene was yellow. The crystals deposited to the bottom of the column because of gravity. Naphthalene had very high concentration in the bottom of the column; therefore, the bottom had many white crystals. In the top of the column, the liquid was squeezed to here, and naphthalene had very low concentration; therefore, it was full of much yellow liquid and little crystals.

The product purity was related to crystal settling velocity and crystal breakage that was controlled by stirring speed, the angle and the pores diameter of sieve plates, the particle sedimentation area, and the number of plates.

1. Temperature and Concentration Profile

The distribution profiles of temperature and concentration along the column axis were measured as shown in Fig. 3(a) and 3(b). Fig. 3(a) was measured after 1 hour of the experiment. Fig. 3(b) was measured when the crystallizer was at a steady state.

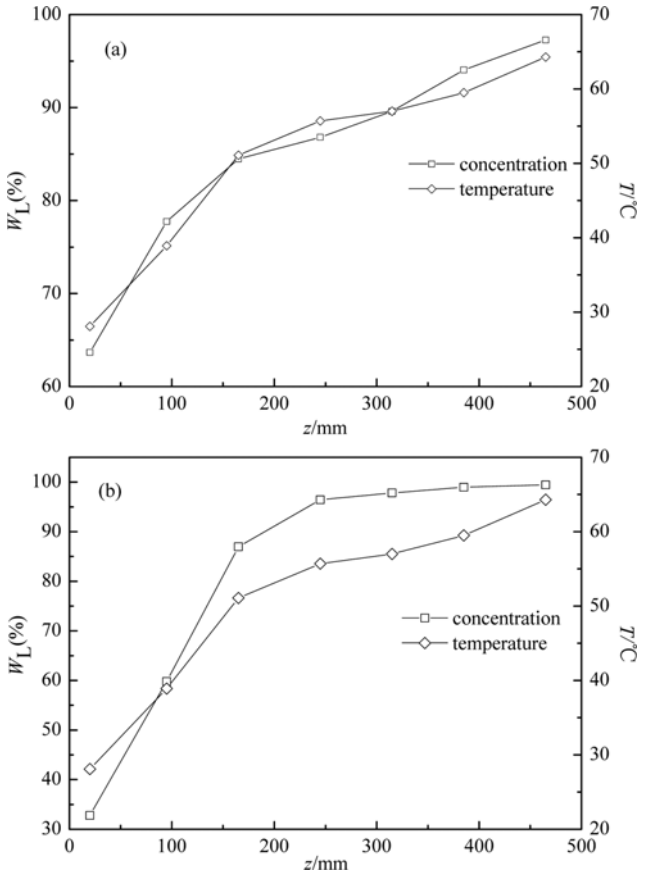

Fig. 3. Temperature and concentration profiles along the axis. (a) The experiment after 1 hour. (b) The crystallizer at steady state.

When the operations reached steady point, two main areas were observed: the crystal bed area and crystal subsidence area. In the crystal bed area the temperature and concentration showed little change, whereas in the crystal subsidence area was observed a change in the temperature and concentration changed. The concentration distribution curves and temperature distribution curves were very similar, which indicated that the crystallizer had reached thermal equilibrium compared to Fig. 3(a) and 3(b). Concentration distribution was related to temperature distribution.

2. Effect of Stirring

Lowering the rotation speed of the scraper can improve the settling; however a higher speed is required to prevent encrustation. In addition, there must be adequate stirring speed to provide good contract between the falling crystals and the reflux melt. Experiments on the effect of stirring and without stirring are shown in Fig. 4(a), and Fig. 4(b) shows the role of stirring by varying the stirring speeds of the shaft.

As shown in Fig. 4(a), in the presence of stirring, significant change in concentration profiles was observed as compared with the extreme case of no stirring. The measured concentration showed a little change along the full column with no stirring. Compared to that of no stirring, the measured concentration has a significant change

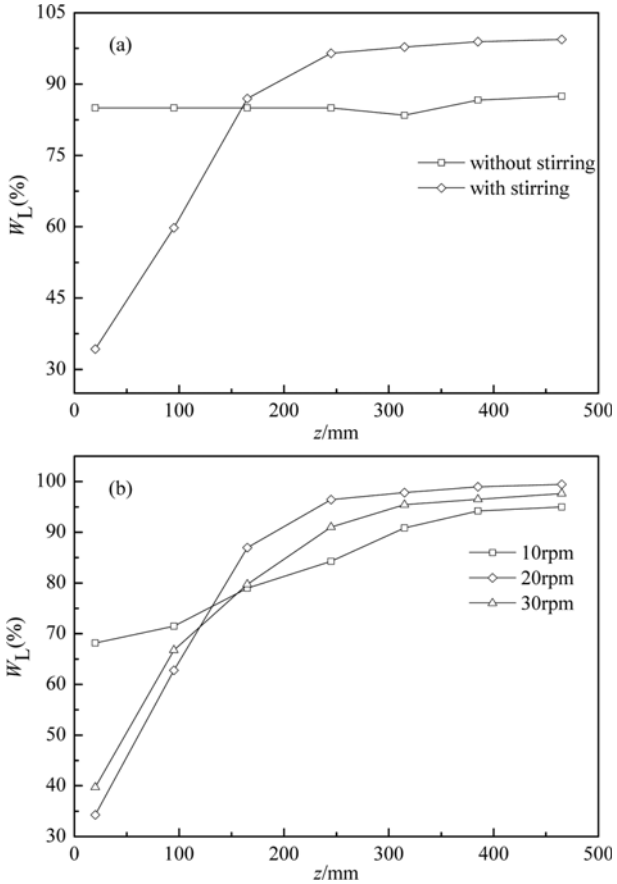

Fig. 4. Effect of stirring on concentration distribution along the column. (a) With or without stirring. (b) Different stirring speed.

along the full column, which this trend can be attributed to the cation of the stirring shaft that provides the crystal bed with gentle agitation, leading to significant improvements in enhancing the mass transfer between the crystal and the melt. On the other hand, the results in Fig. 4(b) suggest that stirring speed beyond a certain value is not necessary for high-purity separation as the product purity is high under the low stirring speed. The optimum rotation speed was determined to be 20 rpm, based on the observed slurry movement and the settling behavior.

3. Effect of the Sieve Plates

To enhance the settling velocity, heat and mass transfer, addition of several sieve plates in the inner of the new crystallizer together with the stirring shaft rotating in the purification inclined is required. The sieve plates enable the crystals to be ground and broken into small particles. Moreover, the sieve plates have the benefit of backwashing and sweating mechanism, which prevents crystal agglomeration in the crystallizer and affects the settlement of crystals.

An experiment was conducted to investigate the role of the crystallizer with or without the sieve plates as shown in Fig. 5. The results showed that the sieve plates can obviously enhance the settling velocity, heat and mass transfer, and broken the crystal to pieces. The measured purity of concentration was also observed to have steady change along the full column.

4. Effect of the Angle of the Sieve Plates

According to the Boycott effect, the angle of the sieve plates has

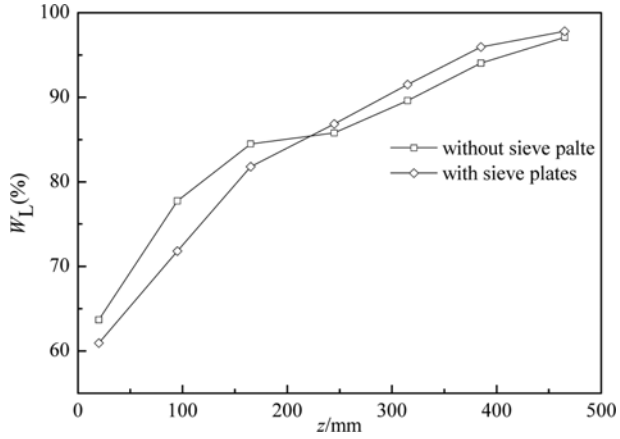

Fig. 5. Effect of with or without sieve plate on concentration distribution along the column.

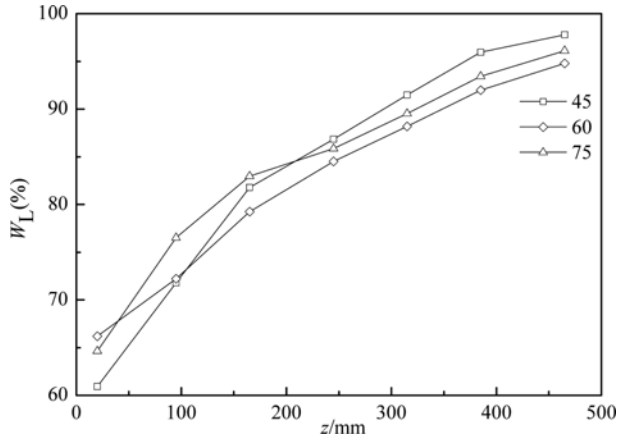

Fig. 6. Effect of the angle of the sieve plate on concentration distribution along the column.

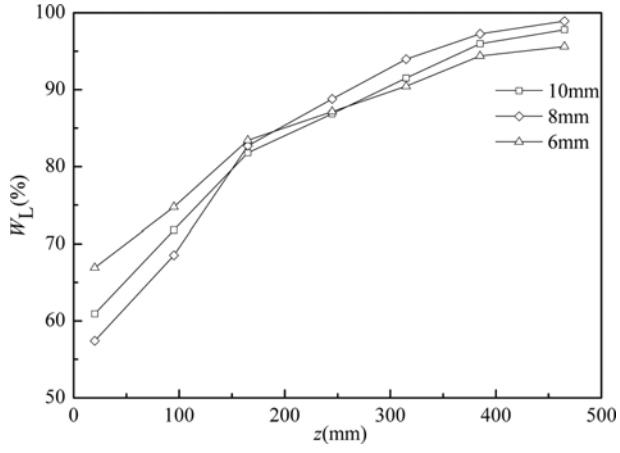

Fig. 7. Effect of the diameter of the pores on concentration distribution along the column.

an effect on crystal settlement. An experiment was conducted to investigate the role of the angle of the sieve plates. The measured purity of concentration profiles is shown in Fig. 6.

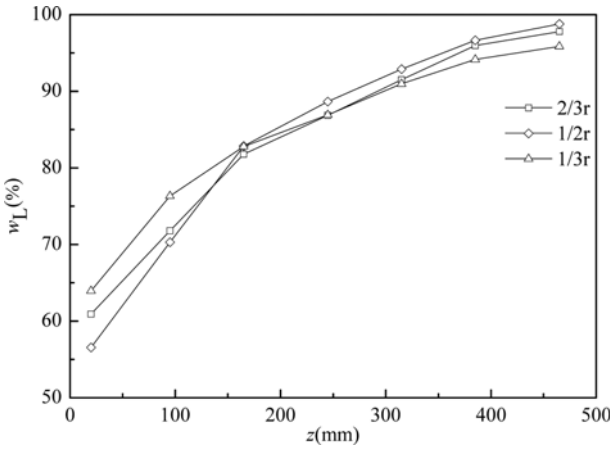

Fig. 8. Effect of the particle sedimentation area on concentration distribution along the column.

From Fig. 7, the effect of the purity was 45°>75°>60°. The optimal angle of the sieve plates was found to be 45°.

5. Effect of the Diameter of the Pores

According to the TNO crystallizer, the porosity of sieve plates could break the big crystal. The pore diameter was the main factor influencing the crystal settlement and crystal breakage effect. A wide diameter had an advantage on crystal settlement, and a smaller diameter had the advantage on crystal breakage. Therefore, consideration should be given when choosing the pores diameter for crystal settlement and crystal breakage. Fig. 8 shows the experiment for the different pore diameter. The effect of the purity was 8 mm >10 mm>6 mm. The optimum diameter of the pore was 8 mm.

6. Effect of the Particle Sedimentation Area

One of the main influencing factors was the width of particle sedimentation area. The width of particle sedimentation area has an advantage on crystal settlement and crystal breakage. It is not good for crystal breakage if the contact area is too big, whereas it is not also good for crystal settlement if the contact area is too small. Hence, depending on whether it is crystal settlement or crystal breakage, the choice of the width particle sedimentation area should be considered. The experiment on the different width of particle sedimentation area is shown in Fig. 9.

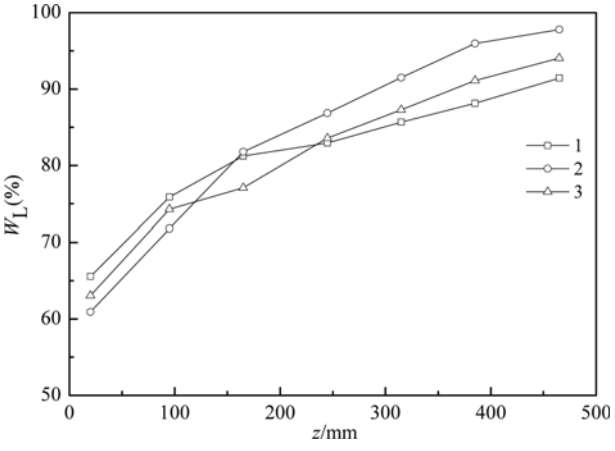

Fig. 9. Effect of the number of plates on concentration distribution along the column.

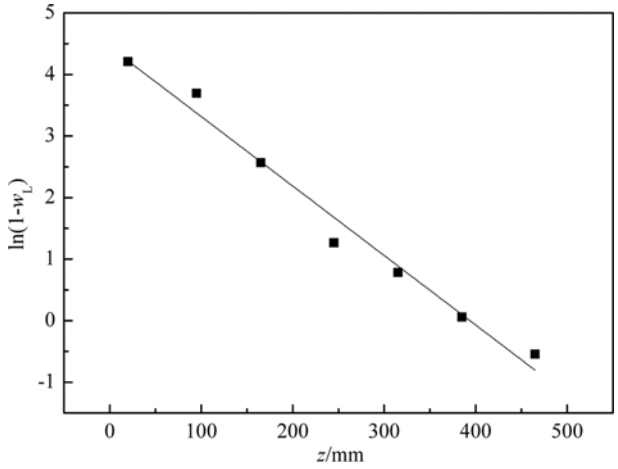

Fig. 10. Impurity profile correlated with simplifies axial dispersion model.

From Fig. 8, the effect of the purity was 0.5 r>0.66 r>0.33 r with the optimal particle sedimentation area being 0.5 r.

7. Effect of the Number of Plates

Another influencing factor is the number of plates. A suitable number of plates has the advantage of crystal settlement and crystal breakage; if the number of plates is less, the crystal settlement function and crystal breakage function cannot reach the purification effect. On the other hand, if there are too many plates, there is an opposite effect on crystal settlement. Choosing the number of plates for this study was very critical. Fig. 10 shows the experiment conducted using a different number of plates.

From Fig. 9, the effect of the purity followed the order: 2 plates> 1 plate>3 plates. The optimal number of plates was found to be two plates.

MODEL VERIFICATION

The concentration of the impurities at different position in the column crystallizer was plotted in semilogarithmic coordinates as shown in Fig. 10. The simplified axial dispersion model was formulated for the purification, which showed a linear fit.

The distribution of impurity concentrations in the purification section exhibited a good linear relationship with position in semilogarithmic coordinates. The data obtained conformed with the predictions of the mathematical model. This agreement with the experimental results illustrates the validity of the model for the new multistage countercurrent melt crystallizer with sieve plates. Also, in the lower layer of the purification product, the purity increases with the crystal settling velocity and crystal breakage, and in the upper layer decreases with the crystal settling velocity and crystal breakage. Two of the influencing factors on the separation and purification performance in the new multistage countercurrent melt crystallizer with sieve plate were crystal settling velocity and crystal breakage. The influencing factors for crystal settling velocity and crystal breakage include stirring, and the sieve plates. Compared to the

behavior of a traditional column crystallizer, the new crystallizer with sieve plates can enhance heat transfer, mass transfer and particles broken capability.

CONCLUSIONS

(1) Crystal settling velocity and crystal breakage were the main factors influencing the separation and purification performance of the new multistage countercurrent melt crystallizer with sieve plates; the influencing factors for crystal settle velocity and crystal breakage were the speed of stirring, the sieve plates, the angle of the sieve plates, the diameter of the pores, particle sedimentation area, and the number of plates.

(2) The sieve plates have an obvious effect for crystal settling velocity and crystal breakage; the optimum stirring speed was determined to be 20 rpm; the optimum angle of the sieve plates was determined to be 45°; the optimum diameter of the pores was determined to be 8 mm; the optimum width of particle sedimentation area was determined to be 0.5 r, and two plates in the crystallizer were shown to be the best.

(3) A simplified axial dispersion model was set up for the purification section and agrees well with the experimental results:

$$\ln\frac{w_L-a}{w_{L0}-a}=\ln\frac{a-w_L}{a-w_{L0}}=-bz$$

For total reflux,

$$\ln\frac{w_L-1}{w_{L0}-1}=\ln\frac{1-w_L}{1-w_{L0}}=-bz$$

or

$$\ln y=\ln y_0-bz$$

(4) The model indicates that the impurity concentration $\ln(1-w_L)$ decreases linearly with the position z in the purification and that the crystal settling velocity and crystal breakage are the dominant factors affecting the separation and purification performance of the crystallizer.

ACKNOWLEDGEMENT

This work was supported by the Special Fund for Basic Scientific Research of Central Colleges (Grant No. ZZ1107).

NOMENCLATURE

A : cross-section area of the crystallizer [m^2]
D_e : coefficient of diffusion [m^2/s]
k : coefficient of purification rate [m^2/s]
M_d : mass flow caused by back-mixing [kg/s]
K_a : the convective diffusion between crystal and melt [m^2/s]
M_k : the mass transfer coefficient between crystal and melt [kg·m^2/s]
r : the inner diameter of crystallizer [mm]
S : flow rate of crystal [kg/s]
L : flow rate of the melt [kg/s]
P : flow rate of product [kg/s]
M : melting rate of the crystals [kg/s]
F : melting rate of the feed [kg/s]
W : melting rate of the residue [kg/s]
w_F : weight fraction of major composition in the feed
v_S : settling velocity of crystal [m/s]
w_P : weight fraction of major composition in the product
w_L : weight fraction of major composition in the melt
w_{L0} : weight fraction of major composition in the melt when z=0
w_S : weight fraction of major composition in the crystal
w_S^* : equilibrium weight fraction of major composition in the crystal
z : position in the column, measured from the freezing section [m]
z_F : feed position in the column [m]
y : weight fraction of impurity composition in the melt
y_0 : weight fraction of impurity composition in the melt when z=0

Greek Letters

θ : time [min]
α : the mass transfer area of the unit volume crystal bed layer [m^3/m^3]
ϕ : volume fraction of crystals
ρ_L : density of melt [kg/m^3]

REFERENCES

1. G. G. Devyatykh, Yu. E. Elliev and A. N. Gur'yanov, *Dokl. Acad. Nauk SSSR*, **204**, 917 (1972).
2. G. G. Devyatykh, V. M. Vorotyntsev, V. M. Malyshev and V. B. Karakisn, *Dokl. Acad. Nauk SSSR*, **297**, 396 (1987).
3. Q. Li, Z. Yi, X. Sun and M. Su, *Korean J. Chem. Eng.*, **27**, 619 (2010).
4. S. K. Myasnikov, A. D. Uteshinsky and N. N. Kulov, T*heor. Found. Chem. Eng.*, **41**, 124 (2007).
5. G. J. Arkenbout, A. V. Kuijk and W. M. *Smit, Chem. Ind.*, **3**, 139 (1973).
6. M. Matsuoka, H. Takiyama and O. Soutome, *Chem. Eng. Res. Des. Trans. Inst. Chem. Eng. A*, **75**, 206 (1997).
7. Boycott A. E. Sedimentation of blood corpuscles [J]. *Nature*, **104**, 532 (1920).
8. K. Funakoshi, H. Uchida, H. Takiyama and M. Matsuoka, *J. Cryst. Growth*, **237**, 2251 (2002).
9. L. Chen, J. Li and M. *Ind. Eng. Chem. Res.*, **45**, 2818 (2006).
10. R. Albertins and J. E. Powers, *AIChE J.*, **15**, 554 (1969).
11. J. D. Henry and J. E. Powers, *AIChE J.*, **16**, 1055 (1970).
12. W. C. Gates and J E. Powers, *AIChE J.*, **16**, 648 (1970).
13. M. Matsuoka, T. Fukuda, Y. Takagi and H. Takiyama, *J. Chem. Eng. Jpn.*, **28**, 562 (1995).
14. M. Matsuoka, T. Fukuda, Y. Takagi and H. Takiyama, *J. Cryst. Growth*, **166**, 1035 (1996).
15. M. Matsuoka and A. Sumitani, *J. Chem. Eng. Jpn.*, **21**, 6 (1988).
16. M. Matsuoka, M. Ohishi and S. Kasama, *J. Chem. Eng. Jpn.*, **19**, 181 (1986).
17. P. Bolsaitis, *Chem. Eng. Sci.*, **24**, 1813 (1969).
18. C. G. Moyers and J. H. Olson, *AIChE J.*, **20**, 1118 (1974).
19. M. R. Player, *Ind. Eng. Chem. Process Dev.*, **8**, 210 (1969).